Journal of Bacteriology

Structural and Functional Characterization of an Orphan ATP-Binding Cassette ATPase Involved in Manganese Utilization and Tolerance in Leptospira spp.

Nadia Benaroudj, Frederick Saul, Jacques Bellalou, Isabelle Miras, Patrick Weber, Vincent Bondet, Gerald L. Murray, Ben Adler, Paula Ristow, Hélène Louvel, Ahmed Haouz and Mathieu Picardeau

J. Bacteriol. **2013, 195(24):5583. DOI: 10.1128/JB.00915-13. Published Ahead of Print 11 October 2013.**

JB
Journals.ASM.org

Structural and Functional Characterization of an Orphan ATP-Binding Cassette ATPase Involved in Manganese Utilization and Tolerance in *Leptospira* spp.

Nadia Benaroudj,[a] Frederick Saul,[b] Jacques Bellalou,[c] Isabelle Miras,[b] Patrick Weber,[b] Vincent Bondet,[c] Gerald L. Murray,[d] Ben Adler,[d] Paula Ristow,[a]* Hélène Louvel,[a]* Ahmed Haouz,[b] Mathieu Picardeau[a]

Institut Pasteur, Unité Biologie des Spirochètes,[a] Plate-Forme de Cristallographie, CNRS-UMR3528,[b] and Plate-Forme Production de Protéines Recombinantes, CNRS-UMR3528,[c] Paris, France; Australian Research Council Centre of Excellence in Structural and Functional Microbial Genomics, Department of Microbiology, Monash University, Clayton, Australia[d]

Pathogenic *Leptospira* species are the etiological agents of the widespread zoonotic disease leptospirosis. Most organisms, including *Leptospira*, require divalent cations for proper growth, but because of their high reactivity, these metals are toxic at high concentrations. Therefore, bacteria have acquired strategies to maintain metal homeostasis, such as metal import and efflux. By screening *Leptospira biflexa* transposon mutants for their ability to use Mn^{2+}, we have identified a gene encoding a putative orphan ATP-binding cassette (ABC) ATPase of unknown function. Inactivation of this gene in both *L. biflexa* and *L. interrogans* strains led to mutants unable to grow in medium in which iron was replaced by Mn^{2+}, suggesting an involvement of this ABC ATPase in divalent cation uptake. A mutation in this ATPase-coding gene increased susceptibility to Mn^{2+} toxicity. Recombinant ABC ATPase of the pathogen *L. interrogans* exhibited Mg^{2+}-dependent ATPase activity involving a P-loop motif. The structure of this ATPase was solved from a crystal containing two monomers in the asymmetric unit. Each monomer adopted a canonical two-subdomain organization of the ABC ATPase fold with an α/β subdomain containing the Walker motifs and an α subdomain containing the ABC signature motif (LSSGE). The two monomers were arranged in a head-to-tail orientation, forming a V-shaped particle with all the conserved ABC motifs at the dimer interface, similar to functional ABC ATPases. These results provide the first structural and functional characterization of a leptospiral ABC ATPase.

Most eukaryotes and prokaryotes require divalent cations (mainly Fe^{2+}, Zn^{2+}, Mn^{2+}, Ni^{2+}, Cu^{2+}, or Co^{2+}) for proper growth and development, as these transition metals are necessary for numerous biological processes (1, 2). Iron, which is present at concentrations in the mM range in *Escherichia coli* (3), has traditionally been considered the most important transition metal in the physiology of bacteria, and several studies have led to a detailed understanding of how iron is acquired by bacterial cells (reviewed in reference 4). However, other divalent cations, such as Zn^{2+}, Cu^{2+}, and Mn^{2+}, also play an important physiological role. Although Mn^{2+} is accumulated to a lesser extent than Fe^{2+} in cells (in the μM range in *E. coli*) (3), it is also involved in major enzymatic reactions and plays an important role in protection from reactive oxygen species (5). In fact, Fe^{2+} and Mn^{2+} are interchangeable in the metal binding site of many metalloenzymes (5, 6). However, the acquisition of Mn^{2+}, as well as its role in the physiology of bacteria, remains poorly understood (7).

Although necessary for bacterial viability, divalent cations can be toxic when present at high concentrations. Therefore, bacteria have acquired strategies to maintain transition metal homeostasis, such as sensing fluctuations in metal cellular content or metal uptake, efflux, and sequestration (8). Metal homeostasis is of great importance for host-pathogen interactions (9). One defensive strategy of the host is to restrict the access of divalent cations to invading bacteria. Another recently discovered strategy is to harness the toxic properties of transition metals to eliminate invading pathogens. Among divalent cations, manganese has recently received attention. Indeed, mutation of the Mn^{2+} uptake system was shown to impair the virulence of several bacterial species, including *Salmonella enterica* serovar Typhimurium (10), *Yersinia pestis* (11), *Bacillus anthracis* (12), *Streptococcus pneumoniae* (13), *Staphylococcus aureus* (14), and *Borrelia burgdorferi* (15). Moreover, exporting excess Mn^{2+} has also proven necessary for infection by *S. pneumoniae* (16), *Xanthomonas oryzae* (17), and *Neisseria meningitidis* (18).

Leptospira spp. are motile, aerobic, chemoorganotrophic spirochetes. Pathogenic *Leptospira* spp. are the causative agents of leptospirosis, a zoonosis of global importance (19, 20). The lack of techniques for genetic manipulation of *Leptospira* spp. has greatly hindered investigation of their physiology, including metal homeostasis and metabolism. Indeed, targeted mutagenesis is extremely inefficient in pathogenic *Leptospira* (20). Our group has developed a system for random transposon mutagenesis using a *mariner* element, *Himar1*, in the saprophyte *Leptospira biflexa* (21) and the pathogen *L. interrogans* (22). This approach allowed the identification of specialized uptake systems for iron (21, 23).

Received 1 August 2013 **Accepted** 2 October 2013

Published ahead of print 11 October 2013

Address correspondence to Mathieu Picardeau, mpicard@pasteur.fr, or Nadia Benaroudj, nadia.benaroudj@pasteur.fr.

* Present address: Paula Ristow, Laboratório de Biologia Molecular Carmen Lemos, Instituto de Biologia, Universidade Federal da Bahia, Salvador, Bahia, Brazil; Hélène Louvel, Génomique des Microorganismes CNRS-UMR7238, Université Pierre et Marie Curie, Paris, France.

Supplemental material for this article may be found at http://dx.doi.org/10.1128/JB.00915-13.

doi:10.1128/JB.00915-13

The transport of metals through the bacterial cytoplasmic membrane is mediated by energy-coupled systems, such as ATP-binding cassette (ABC) and P-type transporters. Proton-coupled transporters, including Nramp (natural resistance associated with macrophage protein) and the resistance and nodulation (RND) and cation diffusion facilitator (CDF) proteins, can also mediate metal uptake (reviewed in reference 8). Analysis of *Leptospira* genomes indicated the presence of putative transporters of the Nramp and ABC families, but none of them has been characterized. Moreover, very little is known about divalent cation acquisition and homeostasis in *Leptospira* spp.

In this study, by screening *L. biflexa* transposon mutants for Mn^{2+}-altered growth, we identified a gene encoding an orphan ABC ATPase of unknown function. We have investigated the functional and structural properties of this new ABC ATPase, encoded by LEPBIa2866 in *L. biflexa* and LIC12079 in *L. interrogans*.

MATERIALS AND METHODS

Bacterial strains and growth conditions. *L. biflexa* serovar Patoc strain Patoc 1, *L. interrogans* serovar Manilae strain L495, and *L. interrogans* serovar Copenhageni strain Fiocruz L1-130 were grown aerobically at 30°C in Ellinghausen-McCullough-Johnson-Harris (EMJH) medium (24). When necessary, kanamycin and/or spectinomycin was added at 40 μg/ml. It should be noted that regular EMJH medium contains $FeSO_4$ and $ZnCl_2$ at concentrations of about 180 and 15 μM, respectively, and that $MnCl_2$ is either absent from this medium or present at concentrations of less than 5 μM. When indicated, $FeSO_4$ was omitted during the preparation of EMJH medium, and when necessary, $MnCl_2$ was added at a final concentration of 100 μM.

Isolation of *Leptospira* mutants with altered manganese phenotypes. Random insertion mutagenesis using the kanamycin-resistant transposon *Himar1* was carried out in *L. biflexa* serovar Patoc strain Patoc 1 and *L. interrogans* serovar Manilae strain L495, as described previously (21, 22). To identify mutants of *L. biflexa* unable to grow in the presence of Mn^{2+}, more than 2,000 random mutants were replica plated onto EMJH medium and iron-deficient EMJH medium containing 100 μM $MnCl_2$. The insertion of a single transposon within each individual clone was confirmed by PCR and Southern blot hybridization, and the position of transposon insertion was determined by direct sequencing of genomic DNA. This allowed us to identify LEPBIa2866 (GI: 91178403) and LEPBIa2071 (GI: 167776217) mutants. LEPBIa2866- and LEPBIa2071-expressing plasmids used in mutant complementation were constructed by PCR amplifying these open reading frames (ORFs) with primer set 2751-2-5′ (5′-ACTCGCTGAAAAATGGGAATTCC-3′) and 2751-2-3′ (5′-TGCGGAGAACACATCGATATTGTC-3′) and primer set 1648-2-5′ (5′-ACAAAGTCCCTAGCCTCGATCCCC-3′) and 1648-2-3′ (5′-TTATGTTCTAACGACTAGTCATTCC-3′), respectively, and ligating the PCR products into the SmaI blunt-ended site of the spectinomycin-resistant *L. biflexa-E. coli* shuttle vector pGSBLe24 (25). Since the LEPBIa2866 ORF is cotranscribed with the upstream LEPBIa2865 ORF, complementation was performed with plasmid pGSBLe24 containing a transcriptional fusion between the *L. interrogans hsp10* (*groES*) promoter and the LEPBIa2866-coding sequence, as described previously (26). Transposon insertion in the *L. interrogans* LEPBIa2866 ortholog (LIC12079, GI: 45657927) was identified in the *L. interrogans* serovar Manilae strain L495 mutant library (22).

Determination of cell viability. *L. biflexa* cells were grown to exponential phase (about 10^8/ml) in EMJH medium and then incubated for 20 h in the absence or presence of 100 μM $MnCl_2$. Cells were then diluted in complete EMJH medium without $MnCl_2$ and plated on solid EMJH medium. After incubation for 1 week at 30°C, colonies were counted and percent survival (as a percentage of the total number of CFU) was calculated as the ratio of the number of CFU for cells incubated in the presence of $MnCl_2$ to that for cells incubated in the absence of $MnCl_2$.

MICs were determined by adding serial 2-fold dilutions of Mn^{2+} to *L. interrogans* cells (about 2×10^6/ml in EMJH medium). Bacteria were incubated at 30°C for 1 week before assessment by dark-field microscopy. The MIC was determined as the point at which growth was inhibited by 50%.

Production and purification of recombinant LIC12079 and the LIC12079-K45A variant. A LIC12079-expressing plasmid was constructed by amplifying the LIC12079 ORF (forward primer, 5′-GGGGACAAGTTTGTACAAAAAAGCAGGCTCGGAAAACCTGTATTTTCAGGGCAAAATCAATTCGTTATTATCCCTAG-3′; reverse primer, 5′-GGGGACCACTTTGTACAAGAAAGCTGGGTTTAATAGGTTCGTTTTTGTTTTGGGATCAC-3′) from *L. interrogans* serovar Copenhageni strain Fiocruz L1-130 and cloning it into the Gateway pDEST17 vector (Life Technologies). A single-mutation variant, LIC12079-K45A, was obtained by replacing the Lys 45 codon by an alanine codon using a QuikChange multisite-directed mutagenesis kit (Agilent Technologies) according to the manufacturer's recommendation and the primer 5′-AAGAAACGGAGCTGG**CGC**AAGTACTCTCGTAAATC-3′ (with the mutated codon indicated in bold). The codon substitution in the LIC12079-K45A variant was confirmed by DNA sequencing (Beckman Coulter Genomics).

E. coli strain BL21(DE3) Δ*dnaK*::*kan* (EN2) (27) was transformed with the pDEST17 expression vector carrying the LIC12079 or the LIC12079-K45A ORF and grown to an absorbance of about 0.7 at 600 nm at 30°C in Luria-Bertani (LB) medium supplemented with 30 μg/ml kanamycin and 100 μg/ml ampicillin. Protein expression was then induced with 1 mM isopropyl-β-D-thiogalactopyranoside (IPTG) for 4 h. After centrifugation, cell pellets were resuspended in buffer A (50 mM NaH_2PO_4, pH 8.0, 300 mM NaCl, 10 mM imidazole, 10% glycerol) and lysed by sonication. The soluble fraction obtained after 60 min centrifugation at 40,000 × *g* at 4°C was loaded on nickel-nitrilotriacetic acid (Ni-NTA) resin (Qiagen) and washed with buffer A. His-tagged proteins were eluted with buffer B (50 mM NaH_2PO_4, pH 8.0, 300 mM NaCl, 250 mM imidazole, 10% glycerol). After elution, His-tagged proteins were dialyzed against buffer C (20 mM Tris-HCl, pH 8.0, 100 mM NaCl, 1 mM dithiothreitol [DTT]) and loaded onto a HiLoad 16/60 Superdex 200 (GE Healthcare) size exclusion chromatography column equilibrated with the same buffer. Elution was performed at a flow rate of 1.0 ml/min. Fractions containing the LIC12079 protein were pooled and concentrated. Protein concentrations were determined with Coomassie Plus protein assay reagent (Thermo Scientific).

The LIC12079 protein used in crystallization experiments was produced in the *E. coli* BLi5 strain [a BL21(DE3)-derived strain that carried a pDIA17 plasmid] (28). Cells were cultivated at 30°C in a microfermentor (Biopod Fogale Nanotech, France) with high-density medium (HDM) containing 100 μg/ml ampicillin and 30 μg/ml chloramphenicol until they reached an absorbance of 20 at 600 nm. Protein expression was induced with 1 mM IPTG for 15 h at 14°C. Cells were harvested and lysed by a French press in 50 mM Tris-HCl, pH 8.2, 100 mM NaCl, and 5 mM imidazole. Purification was performed by nickel immobilized-metal affinity chromatography using a HiTrap Chelating HP column (GE Healthcare), followed by size exclusion chromatographic step using a HiLoad 16/60 Superdex 75 column (GE Healthcare). Fractions containing the LIC12079 protein were pooled and concentrated to 5.2 mg/ml.

Crystallization, X-ray data collection, processing, and refinement. Preliminary crystallization screening was carried out by the sitting-drop vapor diffusion method with a Mosquito (TTP Labtech) automated crystallization system. A 400-nl (1:1) mixture of LIC12079 protein at 5.2 mg/ml and different crystallization solutions (672 commercially available solutions) equilibrated against 150 μl reservoir in Greiner plates was used. The protein crystallized only under conditions containing ammonium sulfate as a precipitant. After extensive screening and optimization, the best crystals were obtained by the hanging-drop method in Linbro plates at 18°C by mixing 1.5 μl of protein solution at 5.2 mg/ml with an equal volume of reservoir solution containing 1.2 M ammonium sulfate and 0.1 M sodium cacodylate, pH 6.5.

Crystals of LIC12079 were flash-cooled in liquid nitrogen using Para-

TABLE 1 Crystallographic parameters and statistics

Parameter[a]	Value(s) for LIC12079[b]
Crystal parameters	
Space group	$P2_12_12_1$
a, *b*, *c* unit cell dimensions (Å)	58.26, 92.51, 130.58
Data collection statistics	
Resolution range (Å)	43.6–1.85 (1.95–1.85)
No. of unique reflections	61,082 (8,809)
Multiplicity	7.5 (6.1)
R_{merge}	0.061 (0.800)
Completeness (%)	100 (100)
$<I/\text{sigma}(I)>$	18.5 (2.3)
Refinement statistics	
Resolution (Å)	43.6–1.85 (1.87–1.85)
R value, working set	0.184 (0.312)
R_{free}	0.220 (0.376)
No. of reflections	59,798 (2,197)
Completeness (%)	99.9 (99.9)
No. of:	
Nonhydrogen atoms	4,506
Protein residues	499
Water molecules	511
SO_4 ions	2
RMSD from ideal	
Bond length (Å)	0.013
Bond angles (°)	1.56

[a] $R_{merge} = \sum_h \sum_l |I_{hl} - <I_h>| / \sum_h \sum_l <I_h>$, where I_{hl} is the *l*th observation of reflection *h*; RMSD, root mean square deviation.
[b] Values in parentheses are for the highest-resolution shell.

tone-paraffin (50%/50%) oil as the cryoprotectant. X-ray diffraction data were collected on beamline PROXIMA-1 at Synchrotron SOLEIL (St. Aubin, France). The diffraction images were integrated with the program XDS (29, 30), and crystallographic calculations were carried out with programs from the CCP4 program suite (31).

The structure was solved by the molecular replacement method with the program Phaser (32), as implemented in the CCP4 program package. The molecular replacement search model was the ABC ATPase SACOL2144 from *S. aureus* (Protein Data Bank [PDB] accession number 2IHY), with 35% sequence identity and 69% sequence similarity to LIC12079. The molecular replacement solution corresponded to two independent molecules in the crystallographic asymmetric unit, with a solvent content (V_s) of 52.4% and a Matthews coefficient (V_m) of 2.58 $Å^3$ Da^{-1} (33). The structure was refined by alternate cycles of restrained maximum likelihood refinement with the program Refmac5 (34). Manual adjustments were made to the model with the Coot program (35). The crystal parameters, data collection statistics, and final refinement statistics are shown in Table 1. All structural figures were generated with the PyMOL program (36).

ATPase activity assay. Purified LIC12079 and LIC12079-K45A were assayed for ATP hydrolysis by monitoring the production of inorganic phosphate at 37°C in 20 mM Tris-HCl, pH 8.0, and 1 mM DTT as described previously (37), using NaH_2PO_4 as a standard.

Protein structure accession number. Atomic coordinates and structure factors have been deposited with the Protein Data Bank with entry code 4HZI.

RESULTS

Isolation of *Leptospira* mutants with Mn^{2+}-deficient growth. The EMJH medium routinely used for the growth of *Leptospira* contains Fe^{2+}, Mg^{2+}, Ca^{2+}, Zn^{2+}, and, in some cases, low concentrations of Mn^{2+} (up to 5 μM). To test the ability of the *L. biflexa* wild-type (WT) strain to use divalent cations other than Fe^{2+}, this metal was omitted from the EMJH medium during medium preparation, and consequently, the medium contained only trace amounts of iron. Various metals were then added to the iron-deficient medium in order to restore leptospiral growth. Mn^{2+} and Zn^{2+} permitted growth at a concentration of 100 μM, whereas the addition of Mg^{2+} (up to 500 μM) or Co^{2+} (up to 1 mM) failed to do so (data not shown). Thus, iron could be exchangeable with Mn^{2+} and Zn^{2+} in *Leptospira*.

In order to identify factors involved in manganese utilization in *Leptospira*, an *L. biflexa* transposon mutant library was screened for Mn^{2+}-altered phenotypes. This allowed the identification of three mutants that were unable to grow in Fe^{2+}-deficient EMJH medium supplemented with Mn^{2+}. In two mutants, the transposon was inserted into the LEPBIa2071 ORF (see Fig. S1A in the supplemental material) that encodes a putative protein displaying similarities to predicted permeases of the major facilitator superfamily (MFS) of *Cytophaga hutchinsonii* (50% identity, 70% similarity), *L. borgpetersenii* (LBL_0798, LBJ_2309; 47% identity, 70% similarity), *L. interrogans* (LMANv1_2290003, LA1081, LIC12590; 47% identity, 69% similarity), and *Nostoc punctiforme* (43% identity, 62% similarity). MFS proteins transport small solutes, including sugars and inorganic ions, in response to chemiosmotic gradients (38). According to the phylogenic classification of the Transport Classification Database (TCDB; http://www.tcdb.org/), LEPBIa2071 could be related to bacterial siderophore exporters EntS (transporter classification number 2.A.1.38.1) and VabS (transporter classification number 2.A.1.38.2). Although most MFS proteins are predicted to contain 12 α-helical transmembrane-spanning segments (TMSs) (38), the *L. biflexa* and *L. interrogans* proteins contain only 10 predicted α-helical TMSs (data not shown).

The third mutant had a transposon insertion in LEPBIa2866, a gene encoding a protein that shares similarity with putative ABC transporter proteins of *L. interrogans* (LMANV1_3710001, LA1724, LIC12079; 40% identity, 61% similarity) and *L. borgpetersenii* (LBL_1280; 40% identity, 60% similarity) (see Fig. S1B in the supplemental material). This level of amino acid identity was consistent with the general genetic relatedness between saprophyte and pathogen strains. Similarities were also found with ORFs from other bacterial species, including *Bacillus subtilis* (38% identity, 56% similarity) and *Streptomyces avermitilis* (37% identity, 56% similarity). Since the *L. interrogans* orthologs exhibited more than 99% nucleotide sequence identity in *L. interrogans* serovars Lai (LA1724), Copenhageni (LIC12079), and Manilae (LMANV1_3710001), we further refer to LIC12079 throughout the text.

L. biflexa WT, LEPBIa2866 mutant, and LEPBIa2071 mutant cells were not able to grow in Fe^{2+}-deficient EMJH medium (data not shown) (23). As shown in Fig. 1A, the addition of 100 μM $MnCl_2$ to Fe^{2+}-deficient EMJH medium did not allow the growth of either the LEPBIa2866 or the LEPBIa2071 mutant but could restore that of WT cells (Fig. 1A). Introduction of a recombinant plasmid harboring the LEPBIa2866 or LEPBIa2071 gene restored the ability of both mutants to use Mn^{2+} as a metal source (Fig. 1B). Notably, both mutants were able to grow in complete EMJH medium, indicating that their manganese-altered phenotype was not due to a general growth defect.

A search of our mutant library of the pathogen *L. interrogans* serovar Manilae (22) identified a mutant with a mutation in the

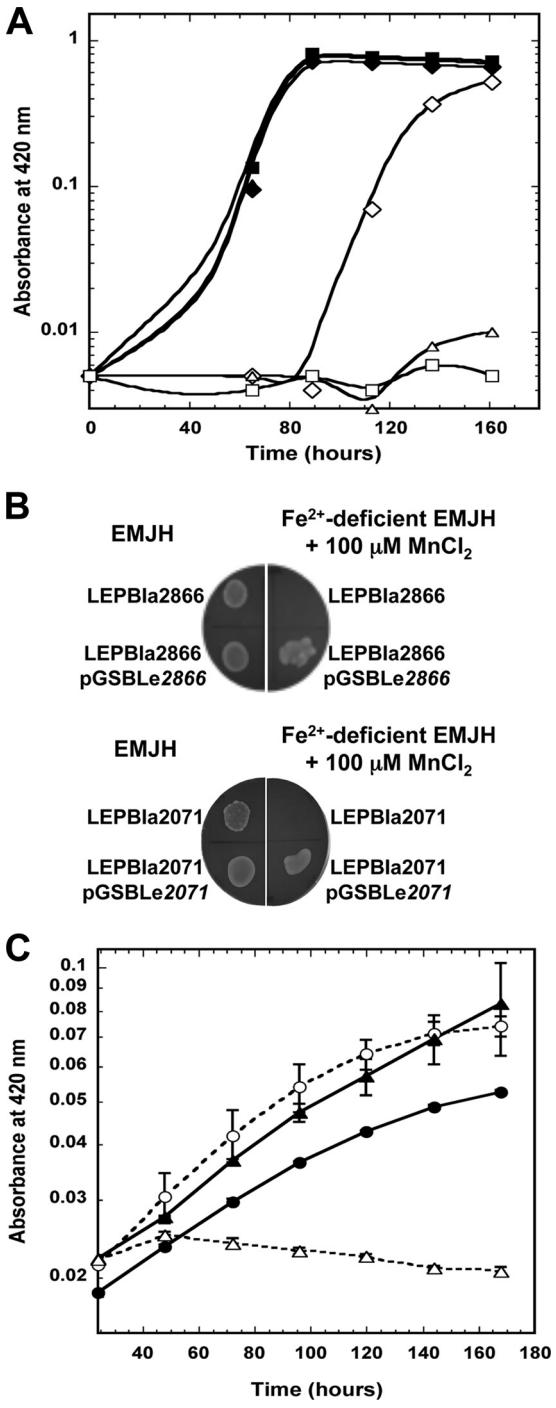

FIG 1 Growth of *Leptospira* in iron-deficient medium in the presence of manganese. (A) Wild-type (diamonds), LEPBIa2071 mutant (triangles), and LEPBIa2866 mutant (squares) strains of *L. biflexa* were grown aerobically at 30°C in EMJH medium (filled symbols) or in Fe^{2+}-deficient EMJH medium supplemented with 100 μM $MnCl_2$ (open symbols). At the indicated times, the absorbance at 420 nm was measured. Data are representative of those from four independent experiments. (B) LEPBIa2866 (top) and LEPBIa2071 (bottom) mutant strains of *L. biflexa*, as well as the equivalent strains containing a replicative LEPBIa2866- or LEPBIa2071-expressing plasmid, were grown for 7 days at 30°C on solid EMJH medium or in Fe^{2+}-deficient EMJH medium with Mn^{2+} added. (C) Wild-type (circles) and LIC12079 mutant (triangles) *L. interrogans* strains were grown aerobically at 30°C in Fe^{2+}-deficient EMJH medium in the presence of 4.5 μM (solid lines, filled symbols) or 100 μM $MnCl_2$ (dashed lines, open symbols). At the indicated times, the absorbance at 420 nm was measured. Results are shown as means ± standard deviations of triplicate samples and are representative of those from two independent experiments. Note that the scale is different than that in panel A.

gene LIC12079, an ortholog of LEPBIa2866. The effect of Mn^{2+} supplementation of Fe^{2+}-deficient EMJH medium on the growth of the LIC12079 mutant was therefore investigated. *L. interrogans* WT cells, as well as the LIC12079 mutant cells, exhibited residual growth in Fe^{2+}-deficient EMJH liquid medium, probably indicating an ability to acquire the trace amounts of Fe^{2+} present in the iron-deficient medium (23). The addition of Mn^{2+} to the Fe^{2+}-deficient medium led to a slight increase in the doubling time of the WT cells, but it did not allow the growth of the LIC12079 mutant (Fig. 1C). These findings indicate that the ABC ATPase encoded by LEPBIa2866 or LIC12079 in *Leptospira* is involved in Mn^{2+} utilization and/or tolerance.

Decreased tolerance to manganese upon inactivation of LEPBIa2866 or LIC12079. In order to determine whether the growth defect in Fe^{2+}-deficient EMJH medium supplemented with Mn^{2+} observed upon inactivation of LEPBIa2866 or LIC12079 was partly due to an inability of these mutants to tolerate the presence of $MnCl_2$, cell survival and growth were measured in complete EMJH medium in the presence of Mn^{2+}. In EMJH medium (containing Fe^{2+}), growth of *L. biflexa* WT and LEPBIa2866 mutant cells was not altered by the presence of 100 μM $MnCl_2$ (Fig. 2A), indicating that the reduced growth of the LEPBIa2866 mutant observed when 100 μM $MnCl_2$ was added to Fe^{2+}-deficient medium could not be explained by a reduced tolerance toward this metal under these conditions. However, higher concentrations of $MnCl_2$ impaired the growth of *L. biflexa* (data not shown). Survival of the WT *L. biflexa* cells was greater than that of LEPBIa2866 mutant cells after 20 h of incubation with 1 mM $MnCl_2$ (Fig. 2B).

The growth of *L. interrogans* was more sensitive to the presence of $MnCl_2$, since the addition of 100 μM $MnCl_2$ to complete EMJH medium reduced its growth. This decrease in growth was even more pronounced in the LIC12079 mutant than in the wild type (Fig. 2C). In addition, cells of the *L. interrogans* WT strain showed significantly higher Mn^{2+} resistance (MIC, 1.25 mM) than LIC12079 mutant cells (MIC, 0.078 mM). These findings indicate that the LIC12079 ORF and its ortholog, LEPBIa2866, are involved in the reduction of Mn^{2+} toxicity in *Leptospira* spp.

LIC12079 is an orphan ABC ATPase. The LIC12079 and its ortholog LEPBIa2866 ORFs are annotated as members of the large ABC transporter family. ABC ATPases couple the energy of ATP hydrolysis with the influx or efflux of a variety of substrates through cellular membranes but also with non-transport-related processes (39). A BLAST analysis of LIC12079 indicated that orthologs of these ORFs are present in the genomes of many *Leptospira* species (saprophyte, intermediate, and pathogen) and also in other bacteria, mostly Gram-positive species.

LIC12079 encodes a 30-kDa protein. Analysis of the primary sequence showed the presence of a single ABC module, but unlike ABC transporters of class 1, this module was not fused to any transmembrane domain (see Fig. S2 in the supplemental material). No gene encoding a protein with a predicted membrane or periplasmic localization was found in the close vicinity of LIC12079. The ORF immediately upstream (LIC12078) encodes a hypothetical protein containing a His/Asp (HD) domain found in

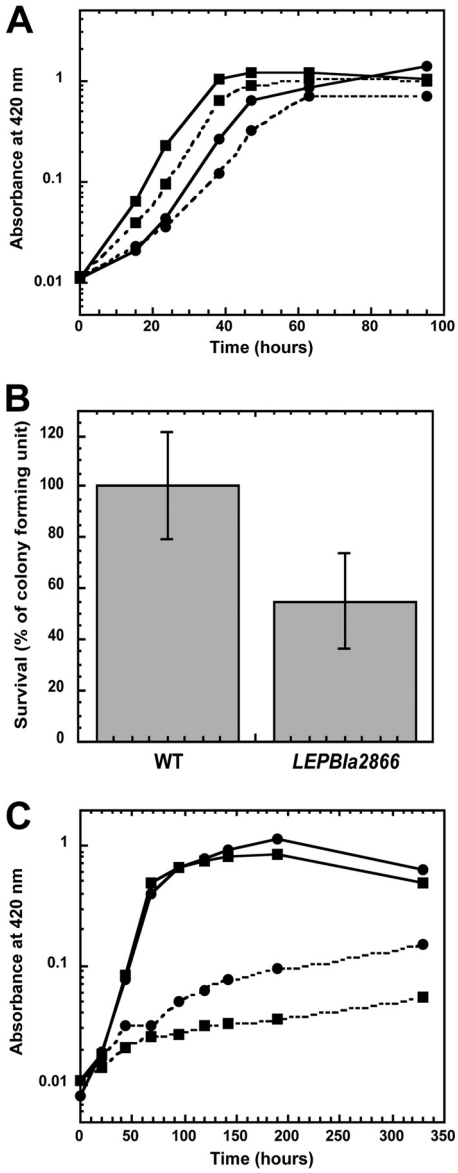

FIG 2 Inactivation of LEPBIa2866 or LIC12079 decreases cell survival in the presence of Mn^{2+}. (A) WT (circles) or LEPBIa2866 mutant (squares) cells of *L. biflexa* were cultivated in complete EMJH medium in the absence (solid lines) or presence (dashed lines) of 100 μM $MnCl_2$ at 30°C. Growth was followed by measuring the absorbance at 420 nm. Data are representative of those from two independent experiments. (B) WT or LEPBIa2866 mutant *L. biflexa* cells were incubated in complete EMJH medium for 20 h in the presence of 1 mM $MnCl_2$ at 30°C. Percent survival was determined as described in Materials and Methods. Results are shown as means ± standard deviations of three independent experiments with a *P* value of 0.05, as determined by the *t* test. (C) Growth of the *L. interrogans* WT (circles) or LIC12079 mutant (squares) in complete EMJH medium in the absence (solid lines) or presence (dashed lines) of 100 μM $MnCl_2$ at 30°C. Growth was monitored by measuring the absorbance at 420 nm. Data are representative of those from three independent experiments.

members of a superfamily of metal-dependent phosphohydrolases (40). It is noteworthy that in *L. biflexa*, transcriptional analysis by reverse transcription-PCR revealed that the LIC12079 ortholog (LEPBIa2866) was cotranscribed with the LIC12078 ortholog (LEPBIa2865) (data not shown). Therefore, LEPBIa2866 and LIC12079 encode an orphan ABC ATPase with no predicted linked transmembrane partner.

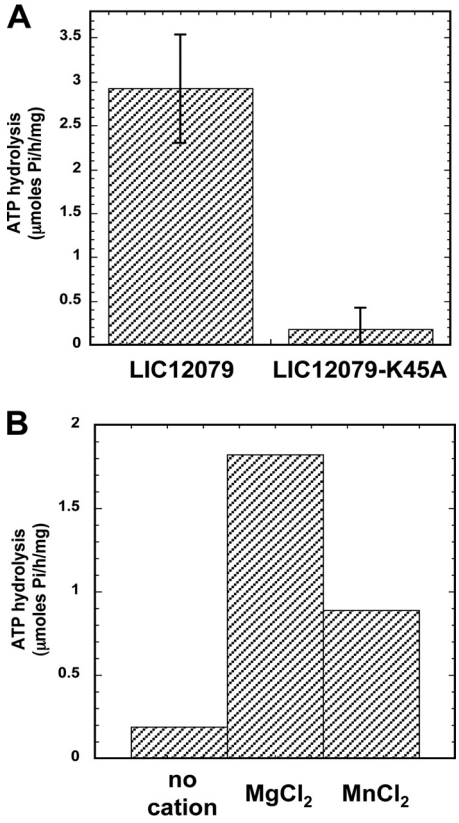

FIG 3 ATP hydrolysis by LIC12079 ABC ATPase. (A) One microgram of purified LIC12079 or the LIC12079-K45A variant was incubated in the presence of 0.1 mM ATP and 10 mM $MgCl_2$. ATP hydrolysis was determined by measuring the production of inorganic phosphate, as described in Materials and Methods. Results are shown as the means ± standard deviations of four independent experiments. (B) One microgram of purified LIC12079 was incubated with 0.1 mM ATP in the absence or presence of 10 mM the indicated cation. ATP hydrolysis was measured as described for panel A. Data are the means of two independent experiments.

The primary sequences of LIC12079 and LEPBIa2866 were aligned with the primary sequence of the glucose transporter of *Sulfolobus solfataricus* (GlcV), a well-characterized ABC transporter. The sequence of LIC12079 exhibited all typical ABC ATPase motifs (41) (see Fig. S2 in the supplemental material), including the Walker A (GRNGAGKS) and Walker B (FLIMDE) motifs of a P-loop nucleoside triphosphatase (NTPase) (42), a putative Q-loop sequence (QQENSIQR) located between the Walker motifs, and a putative H loop (THR) located downstream from the Walker B motif. An LSSGE sequence was found upstream of the Walker B motif. The LSSGE sequence corresponds to the ABC transporter family LSGGQ signature (43), a motif unique to ABC ATPases that, together with the Walker motifs, interacts with ATP.

The ability of recombinant LIC12079 protein to hydrolyze ATP was tested. To avoid contamination by two other major *E. coli* ATPases, the DnaK and GroEL/GroES chaperones, recombinant LIC12079 was produced in a BL21(DE3) Δ*dnaK* strain (27), and the purification protocol contained a size exclusion chromatography step to separate the 30-kDa LIC12079 from the 870-kDa GroEL/GroES complex. The purified wild-type LIC12079 exhibited ATPase activity (Fig. 3A). Replacing the lysine residue of the

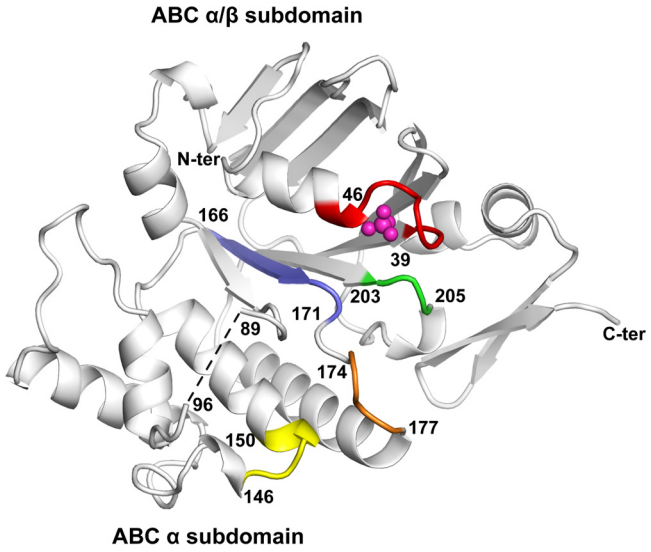

FIG 4 Structure of the LIC12079 ABC ATPase. The three-dimensional structure of the LIC12079 monomer (chain A) is represented by a ribbon diagram. The canonical ABC ATPase motifs are indicated in different colors with the corresponding amino acid numbers: the Walker A motif (or P loop) in red, the Walker B motif in blue, the H motif in green, the D loop in orange, and the ABC signature motif in yellow. Dashed lines indicate the disordered segment of the polypeptide chain in the α subdomain. The bound sulfate ion is represented as purple spheres. N-ter and C-ter, N terminus and C terminus, respectively.

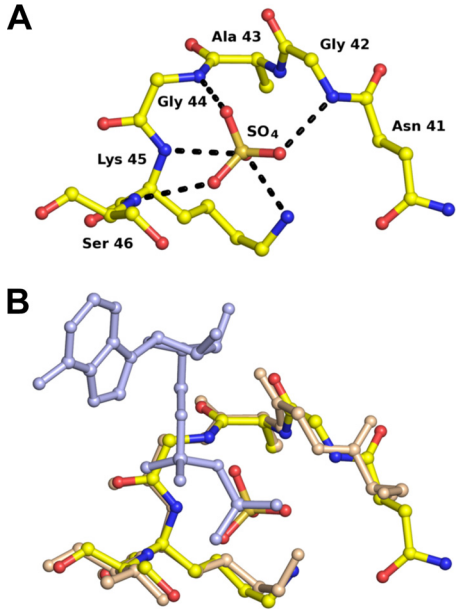

FIG 5 Representation of residues Asn41 to Ser46 of the Walker A motif in LIC12079. (A) Hydrogen bond interactions of the bound sulfate ion with the Walker A motif in LIC12079 are represented by dashed lines. Carbon atoms are shown in yellow, oxygen atoms in red, nitrogen atoms in blue, and sulfur atoms in gold. (B) Comparison of residues Asn41 to Ser46 of the Walker A motif in LIC12079 with the equivalent residues (Ser40 to Thr45) in *S. solfataricus* ABC ATPase GlcV (PDB accession number 1OXU). The ABC α/β subdomain of GlcV was superimposed with the corresponding residues of LIC12079. GlcV is shown in gold, and its bound ADP is in light blue. LIC12079 and its bound sulfate ion are colored as described for panel A.

Walker A motif (Lys45 in LIC12079), known to be involved in ATP hydrolysis, by alanine resulted in significantly decreased ATPase activity (Fig. 3A).

As expected for a P-loop NTPase, the ability of LIC12079 to hydrolyze ATP depended on the presence of Mg^{2+} (Fig. 3B). Despite a putative role of this ABC ATPase in Mn^{2+} uptake or utilization, this cation did not support LIC12079 ATPase activity in a manner comparable to that of Mg^{2+}. ATPase hydrolysis by LIC12079 was also increased in the presence of sodium or potassium salts (data not shown). These findings demonstrate that the recombinant LIC12079 protein was purified in a native conformation exhibiting ATPase activity.

Overall crystal structure. In order to gain insight into the structural organization of the ABC ATPase LIC12079, its crystal structure was determined. This protein crystallized in the absence of nucleotide with two independent molecules in the asymmetric unit. The final model consisted of residues 4 to 262 for both polypeptide chains, with no visible density from residues Gln90 to Gln95 in both chains or from residues Phe109 to Arg116 in chain B. Both polypeptides adopted identical folding and could be closely superimposed, with an overall root mean square deviation of 0.58 Å in alpha-carbon positions. A bound sulfate ion was present in each monomer.

Each ABC ATPase monomer adopted a two-subdomain organization of the canonical ABC ATPase fold (Fig. 4). The ABC α/β subdomain of LIC12079 (residues 4 to 86 and 164 to 228) displayed a central α helix packed between two β sheets, a three-stranded antiparallel sheet, and a five-stranded parallel sheet followed by an additional antiparallel β strand. In this domain, the Walker A motif folded into the canonical loop-helix structure and the Walker B motif was located in the parallel β sheet. The ABC α subdomain (residues 87 to 163) contained four α helices. The ABC signature motif (LSSGE in LIC12079) was contained in a central helix. The highly exposed Q loop (Gln89-Arg96) connecting the two subdomains was disordered, displaying weak discontinuous electron density in both chains in the crystal structure. This disorder could be due to the absence of nucleotide in the active site. An additional α/β structure (residues 229 to 262) was present at the C terminus of the α/β ABC subdomain.

Close structural similarity with the ABC ATPase domain of GlcV from *S. solfataricus* in its ADP-bound form was observed (44) (see Fig. S3 in the supplemental material). In LIC12079, the Walker A motif and the strictly conserved residues Asp170 and Glu171 (the putative catalytic base) at the C terminus of the Walker B motif were present with a conserved spatial orientation. Other structural motifs, the D loop (Ser174-Asp177) and the H loop (Thr203-His204-Arg205), could be closely superimposed with the corresponding residues in the GlcV ATPase structure. The ABC signature motif (LSSGE in LIC12079), partially exposed to solvent at the beginning of the central α helix in the ABC α subdomain, also adopted a similar conformation in the superimposed structures.

Attempts to determine the structure of LIC12079 in complex with AMP, ADP, or ATP by cocrystallization or soaking were unsuccessful, possibly due to the presence of a bound sulfate ion (from the crystallization solution) at the nucleotide binding site (Fig. 5A). The Walker A motif of LIC12079 could be closely superimposed with the corresponding motif in the ADP-bound structure of GlcV from *S. solfataricus* (Fig. 5B). Indeed, residues

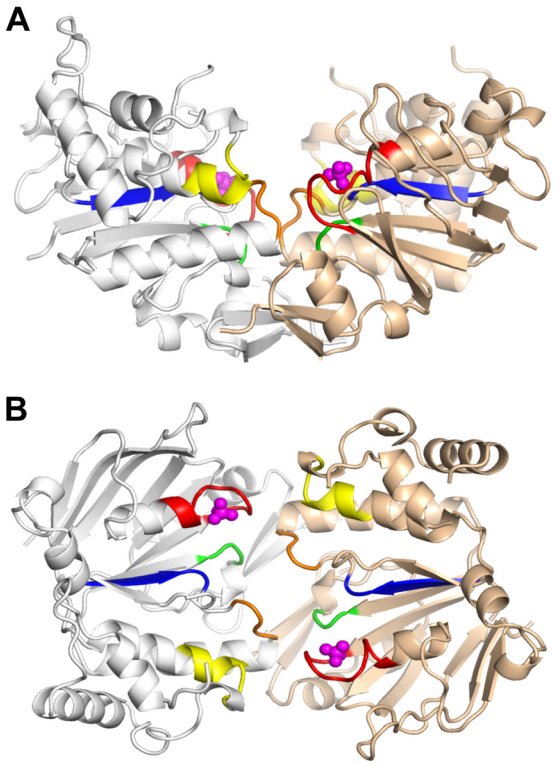

FIG 6 Structure of the LIC12079 ABC ATPase dimer. Side (A) and top (B) views of the V-shaped LIC12079 dimer (chains A and B, represented in silver and in gold, respectively) are shown. The conserved ABC ATPase motifs are indicated in different colors, as described in the legend to Fig. 4, and the two bound sulfate ions are represented as purple spheres.

Gly42, Gly44, Lys45, and Ser46 in the Walker A motif, which could make hydrogen bonds with the β phosphate in the ATP-binding site, were strictly conserved in spatial orientation with the corresponding residues in GlcV (see also Fig. S2 and S3 in the supplemental material). The equivalent residues in LIC12079 interacted with a sulfate ion located at the equivalent position of the ADP β-phosphate group in the GlcV ADP-bound form (Fig. 5B). By homology with other ABC transporters (45), the adenine moiety of the nucleotide could be stabilized by interactions with the side chain of Tyr14 in LIC12079 (data not shown).

The two LIC12079 monomers were arranged in a head-to-tail orientation, forming a V-shaped particle (Fig. 6A). The interface between the two molecules included two C-terminal β strands and the two conserved D and H loops (Fig. 6B). All the other ABC conserved motifs were also located near the interface between the two monomers, with the Walker A and B motifs of each monomer facing the C loop of the other. This arrangement is similar to that of other ABC ATPase dimers (46). Interactions between the two monomers were hydrophobic and electrostatic, with a buried surface area of 2,960 Å^2, as calculated by the European Bioinformatics Institute PISA web-based server (47). Analysis by dynamic light scattering and size exclusion chromatography indicated a dimeric self-association of the protein in solution (data not shown).

DISCUSSION

Manganese is an important divalent cation metal that has a dual effect on cell growth; it can be a nutrient as well as a toxic element. In the present study, we identified and characterized a novel ABC ATPase in *Leptospira* whose inactivation led to the decreased growth of the fast-growing saprophyte *L. biflexa* and the slow-growing pathogen *L. interrogans* when Fe^{2+} was replaced by Mn^{2+} and led to reduced survival in the presence of toxic concentrations of Mn^{2+}. The observed phenotypes differed slightly between the two leptospiral species. In *L. biflexa*, Mn^{2+} could restore the growth of wild-type cells in the absence of Fe^{2+} but not that of LEPBIa2866 ABC ATPase mutant cells. Even though Mn^{2+} was toxic for this strain when used at higher concentrations, 100 μM $MnCl_2$ was not lethal (Fig. 2), and the inability of *L. biflexa* LEPBIa2866 mutant cells to grow in Fe^{2+}-deficient medium in the presence of Mn^{2+} could therefore be explained by an inability to take up Mn^{2+}. When iron was not added to the medium, *L. interrogans* cells still exhibited residual growth. Addition of 100 μM $MnCl_2$, a toxic concentration for *L. interrogans* (Fig. 2), greatly reduced the growth of the ABC ATPase mutant, perhaps reflecting a lower tolerance of these cells toward Mn^{2+}. Under these conditions, the sensitivity of *L. interrogans* to Mn^{2+} precluded the discrimination between Mn^{2+} uptake and sensitivity.

The difference in phenotypes between *L. biflexa* and *L. interrogans* mutants could be explained if the ABC ATPase encoded by LEPBIa2866 or LIC12079 is involved in both the uptake and the efflux of Mn^{2+}, implying interaction of a single ABC ATPase with different transmembrane components involved in the uptake and the export of Mn^{2+}. Examples of a single ABC ATPase component serving several transporter systems have recently been reported in the literature (48–50), although to our knowledge not with both import and export systems. Alternatively, the LEPBIa2866 or LIC12079 ATPase could serve in a non-transport-related process that allows utilization of Mn^{2+}. Further experiments will be necessary to define the precise role of this ATPase in Mn^{2+} transport, tolerance, or utilization.

The *Leptospira* ATPase described here possesses all the canonical motifs of ABC ATPases (39). In this study, we have experimentally demonstrated that LIC12079 displays ATPase activity and exhibits the typical ABC ATPase structural architecture. A BLAST analysis showed that it shares close sequence homology with mostly uncharacterized ABC ATPases that are predicted to energize the transport of solutes, including iron, molybdenum, sulfate, and amino acids. LIC12079 has been classified as a member of the YLU ABC family in the phylogenic and functional classification of ABC systems (http://www.pasteur.fr/abcisse). This family includes orphan ABC ATPases with no defined function or substrate, and no member of this family has been characterized so far. Our study therefore provides the first characterization of a YLU family member and establishes experimental evidence that members of this ABC ATPase family might be involved in divalent cation utilization and tolerance.

The transmembrane component that could mediate the transport energized by the LEPBIa2866 or LIC12079 ATPase is still unknown, and no gene encoding a predicted transmembrane protein could be identified in the close vicinity of these ORFs in *L. biflexa* or *L. interrogans*. It is noteworthy that comparing the chromosomal loci of LEPBIa2866 or LIC12079 orthologs in all the genomes available in the databases showed that this organization is conserved in saprophyte, intermediate, and pathogen *Leptospira* species. Similar to the findings for *Leptospira*, the *S. aureus* LIC12079 homolog, SACOL2144, was not found in the vicinity of genes encoding membrane proteins. Interestingly, another trans-

poson insertion identified during the screening of the *L. biflexa* mutant library was in ORF LEPBIa2071, encoding a putative permease of the MFS transporter family. MFS permeases use the proton motive force rather than ATP hydrolysis as an energy source for solute transport (38). Recently, a functional interplay between an MFS permease and an ABC ATPase in macrolide efflux has been described (51). It would be interesting to investigate whether a possible functional relationship exists between LEPBIa2866 ATPase and the permease encoded by LEPBIa2071 in divalent cation transport and to study the specificity of the transport system energized by the ABC ATPase LEPBIa2866 or LIC12079, which might not be restricted to Mn^{2+}.

It is interesting to note that the ORFs immediately upstream of the ABC ATPase genes LEPBIa2866 (in *L. biflexa*) and LIC12079 (in *L. interrogans*) encode putative phosphatases from the HD family (LEPBIa2865 and LIC12078, respectively). Similarly, the closest structurally related ortholog of LIC12079, the *S. aureus* SACOL2144, is adjacent to an ORF encoding a haloacid dehalogenase (HAD)-like phosphatase (SACOL2143). Since all these phosphatases usually require divalent cations for activity (40), one can speculate that the LEPBIa2866 and LIC12079 ATPases are involved in either the import or incorporation of divalent cations used by the upstream HD phosphatase.

Our study has led to the determination of the crystal structure of an orphan ABC ATPase dimer. ABC ATPases are subject to nucleotide-dependent conformational changes (52). In the ATP-bound form of the dimer, two ABC monomers form a closed interface allowing ATP to interact with the P loop of one ABC ATPase monomer and the ABC signature motif of the second monomer. ATP hydrolysis leads to a conformation with a wider interface between the two monomers. The crystal structure determined in this study showed the two LIC12079 monomers arranged as a dimer with a wide groove at the interface, consistent with the typical conformation of an ADP-bound or nucleotide-free ABC ATPase dimer.

To date, less than 0.03% of all structures available in the Protein Data Bank are of leptospiral origin. In this study, we report the first structure of an ABC ATPase from *Leptospira*. In addition, by presenting a functional characterization of an orphan ABC ATPase of the YLU family in *Leptospira* spp., this study contributes to a better understanding of the physiology of these bacteria.

ACKNOWLEDGMENTS

P.R. was supported by CAPES (Brasil) and a Fiocruz-Pasteur grant. H.L. was supported by a grant from the Région Ile-de-France. G.L.M. was a recipient of an NHMRC Peter Doherty Fellowship. Aspects of the work were supported by the Australian Research Council and the National Health and Medical Research Council, the Institut Pasteur, and the French Ministry of Research (ANR-08-MIE-018).

We acknowledge SOLEIL for provision of synchrotron radiation facilities, and we thank the staff of beamline PROXIMA-1 for assistance. We are grateful to O. Chesneau, E. Dassa, A. Eshghi, G. Karimova, A. Lambert, and A. Ullmann for valuable comments on the manuscript.

REFERENCES

1. **Andreini C, Bertini I, Cavallaro G, Holliday GL, Thornton JM.** 2008. Metal ions in biological catalysis: from enzyme databases to general principles. J. Biol. Inorg. Chem. **13:**1205–1218.
2. **Barondeau DP, Getzoff ED.** 2004. Structural insights into protein-metal ion partnerships. Curr. Opin. Struct. Biol. **14:**765–774.
3. **Outten CE, O'Halloran TV.** 2001. Femtomolar sensitivity of metalloregulatory proteins controlling zinc homeostasis. Science **292:**2488–2492.
4. **Braun V, Hantke K.** 2011. Recent insights into iron import by bacteria. Curr. Opin. Chem. Biol. **15:**328–334.
5. **Jakubovics NS, Jenkinson HF.** 2001. Out of the iron age: new insights into the critical role of manganese homeostasis in bacteria. Microbiology **147:**1709–1718.
6. **Fitsanakis VA, Zhang N, Garcia S, Aschner M.** 2010. Manganese (Mn) and iron (Fe): interdependency of transport and regulation. Neurotox. Res. **18:**124–131.
7. **McEwan AG.** 2009. New insights into the protective effect of manganese against oxidative stress. Mol. Microbiol. **72:**812–814.
8. **Ma Z, Jacobsen FE, Giedroc DP.** 2009. Coordination chemistry of bacterial metal transport and sensing. Chem. Rev. **109:**4644–4681.
9. **Botella H, Stadthagen G, Lugo-Villarino G, de Chastellier C, Neyrolles O.** 2012. Metallobiology of host-pathogen interactions: an intoxicating new insight. Trends Microbiol. **20:**106–112.
10. **Zaharik ML, Cullen VL, Fung AM, Libby SJ, Kujat Choy SL, Coburn B, Kehres DG, Maguire ME, Fang FC, Finlay BB.** 2004. The Salmonella enterica serovar Typhimurium divalent cation transport systems MntH and SitABCD are essential for virulence in an Nramp1G169 murine typhoid model. Infect. Immun. **72:**5522–5525.
11. **Bearden SW, Perry RD.** 1999. The Yfe system of Yersinia pestis transports iron and manganese and is required for full virulence of plague. Mol. Microbiol. **32:**403–414.
12. **Gat O, Mendelson I, Chitlaru T, Ariel N, Altboum Z, Levy H, Weiss S, Grosfeld H, Cohen S, Shafferman A.** 2005. The solute-binding component of a putative Mn(II) ABC transporter (MntA) is a novel Bacillus anthracis virulence determinant. Mol. Microbiol. **58:**533–551.
13. **Marra A, Lawson S, Asundi JS, Brigham D, Hromockyj AE.** 2002. In vivo characterization of the psa genes from Streptococcus pneumoniae in multiple models of infection. Microbiology **148:**1483–1491.
14. **Horsburgh MJ, Wharton SJ, Cox AG, Ingham E, Peacock S, Foster SJ.** 2002. MntR modulates expression of the PerR regulon and superoxide resistance in Staphylococcus aureus through control of manganese uptake. Mol. Microbiol. **44:**1269–1286.
15. **Ouyang Z, He M, Oman T, Yang XF, Norgard MV.** 2009. A manganese transporter, BB0219 (BmtA), is required for virulence by the Lyme disease spirochete, Borrelia burgdorferi. Proc. Natl. Acad. Sci. U. S. A. **106:**3449–3454.
16. **Rosch JW, Gao G, Ridout G, Wang YD, Tuomanen EI.** 2009. Role of the manganese efflux system mntE for signalling and pathogenesis in Streptococcus pneumoniae. Mol. Microbiol. **72:**12–25.
17. **Li C, Tao J, Mao D, He C.** 2011. A novel manganese efflux system, YebN, is required for virulence by Xanthomonas oryzae pv. oryzae. PLoS One **6:**e21983. doi:10.1371/journal.pone.0021983.
18. **Veyrier FJ, Boneca IG, Cellier MF, Taha MK.** 2011. A novel metal transporter mediating manganese export (MntX) regulates the Mn to Fe intracellular ratio and Neisseria meningitidis virulence. PLoS Pathog. **7:**e1002261. doi:10.1371/journal.ppat.1002261.
19. **Faine SB, Adler B, Bolin C, Perolat P.** 1999. Leptospira and leptospirosis, 2nd ed. MediSci, Melbourne, Australia.
20. **Ko AI, Goarant C, Picardeau M.** 2009. Leptospira: the dawn of the molecular genetics era for an emerging zoonotic pathogen. Nat. Rev. Microbiol. **7:**736–747.
21. **Louvel H, Saint Girons I, Picardeau M.** 2005. Isolation and characterization of FecA- and FeoB-mediated iron acquisition systems of the spirochete *Leptospira biflexa* by random insertional mutagenesis. J. Bacteriol. **187:**3249–3254.
22. **Murray GL, Morel V, Cerqueira GM, Croda J, Srikram A, Henry R, Ko AI, Dellagostin OA, Bulach DM, Sermswan R, Adler B, Picardeau M.** 2009. Genome-wide transposon mutagenesis in pathogenic Leptospira spp. Infect. Immun. **77:**810–816.
23. **Louvel H, Bommezzadri S, Zidane N, Boursaux-Eude C, Creno S, Magnier A, Rouy Z, Medigue C, Girons IS, Bouchier C, Picardeau M.** 2006. Comparative and functional genomic analyses of iron transport and regulation in *Leptospira* spp. J. Bacteriol. **188:**7893–7904.
24. **Ellinghausen HC, McCullough WG.** 1965. Nutrition of *Leptospira pomona* and growth of 13 other serotypes: fractionation of oleic albumin complex and a medium of bovine albumin and polysorbate 80. Am. J. Vet. Res. **26:**45–51.
25. **Bourhy P, Frangeul L, Couve E, Glaser P, Saint Girons I, Picardeau M.** 2005. Complete nucleotide sequence of the LE1 prophage from the spirochete *Leptospira biflexa* and characterization of its replication and partition functions. J. Bacteriol. **187:**3931–3940.

26. **Bauby H, Saint Girons I, Picardeau M.** 2003. Construction and complementation of the first auxotrophic mutant in the spirochaete *Leptospira meyeri*. Microbiology **149:**689–693.
27. **Ratelade J, Miot MC, Johnson E, Betton JM, Mazodier P, Benaroudj N.** 2009. Production of recombinant proteins in the lon-deficient BL21(DE3) strain of Escherichia coli in the absence of the DnaK chaperone. Appl. Environ. Microbiol. **75:**3803–3807.
28. **Leon RG, Munier-Lehmann H, Barzu O, Baudin-Creuza V, Pietri R, Lopez-Garriga J, Cadilla CL.** 2004. High-level production of recombinant sulfide-reactive hemoglobin I from Lucina pectinata in Escherichia coli. High yields of fully functional holoprotein synthesis in the BLi5 E. coli strain. Protein Expr. Purif. **38:**184–195.
29. **Kabsch W.** 2010. Integration, scaling, space-group assignment and post-refinement. Acta Crystallogr. D Biol. Crystallogr. **66:**133–144.
30. **Kabsch W.** 2010. Xds. Acta Crystallogr. D Biol. Crystallogr. **66:**125–132.
31. **Winn MD, Ballard CC, Cowtan KD, Dodson EJ, Emsley P, Evans PR, Keegan RM, Krissinel EB, Leslie AG, McCoy A, McNicholas SJ, Murshudov GN, Pannu NS, Potterton EA, Powell HR, Read RJ, Vagin A, Wilson KS.** 2011. Overview of the CCP4 suite and current developments. Acta Crystallogr. D Biol. Crystallogr. **67:**235–242.
32. **McCoy AJ, Grosse-Kunstleve RW, Adams PD, Winn MD, Storoni LC, Read RJ.** 2007. Phaser crystallographic software. J. Appl. Crystallogr. **40:**658–674.
33. **Matthews BW.** 1968. Solvent content of protein crystals. J. Mol. Biol. **33:**491–497.
34. **Murshudov GN, Skubak P, Lebedev AA, Pannu NS, Steiner RA, Nicholls RA, Winn MD, Long F, Vagin AA.** 2011. REFMAC5 for the refinement of macromolecular crystal structures. Acta Crystallogr. D Biol. Crystallogr. **67:**355–367.
35. **Emsley P, Cowtan K.** 2004. Coot: model-building tools for molecular graphics. Acta Crystallogr. D Biol. Crystallogr. **60:**2126–2132.
36. **DeLano WL.** 2010. The Pymol molecular graphics system, version 1.3r1. Schrödinger LLC, New York, NY.
37. **Ames BN.** 1966. Assay of inorganic phosphate, total phosphate and phosphatases. Methods Enzymol. **8:**115–118.
38. **Pao SS, Paulsen IT, Saier MH.** 1998. Major facilitator superfamily. Microbiol. Mol. Biol. Rev. **62:**1–34.
39. **Davidson AL, Dassa E, Orelle C, Chen J.** 2008. Structure, function, and evolution of bacterial ATP-binding cassette systems. Microbiol. Mol. Biol. Rev. **72:**317–364.
40. **Aravind L, Koonin EV.** 1998. The HD domain defines a new superfamily of metal-dependent phosphohydrolases. Trends Biochem. Sci. **23:**469–472.
41. **Dassa E.** 2011. Natural history of ABC systems: not only transporters. Essays Biochem. **50:**19–42.
42. **Walker JE, Saraste M, Runswick MJ, Gay NJ.** 1982. Distantly related sequences in the alpha- and beta-subunits of ATP synthase, myosin, kinases and other ATP-requiring enzymes and a common nucleotide binding fold. EMBO J. **1:**945–951.
43. **Ames GF, Mimura CS, Holbrook SR, Shyamala V.** 1992. Traffic ATPases: a superfamily of transport proteins operating from Escherichia coli to humans. Adv. Enzymol. Relat. Areas Mol. Biol. **65:**1–47.
44. **Verdon G, Albers SV, Dijkstra BW, Driessen AJM, Thunnissen A.** 2003. Crystal structures of the ATPase subunit of the glucose ABC transporter from Sulfolobus solfataricus: nucleotide-free and nucleotide-bound conformations. J. Mol. Biol. **330:**343–358.
45. **Ambudkar SV, Kim IW, Xia D, Sauna ZE.** 2006. The A-loop, a novel conserved aromatic acid subdomain upstream of the Walker A motif in ABC transporters, is critical for ATP binding. FEBS Lett. **580:**1049–1055.
46. **Hollenstein K, Dawson RJ, Locher KP.** 2007. Structure and mechanism of ABC transporter proteins. Curr. Opin. Struct. Biol. **17:**412–418.
47. **Krissinel E, Henrick K.** 2007. Inference of macromolecular assemblies from crystalline state. J. Mol. Biol. **372:**774–797.
48. **Ferreira MJ, Sa-Nogueira I.** 2010. A multitask ATPase serving different ABC-type sugar importers in Bacillus subtilis. J. Bacteriol. **192:**5312–5318.
49. **Marion C, Aten AE, Woodiga SA, King SJ.** 2011. Identification of an ATPase, MsmK, which energizes multiple carbohydrate ABC transporters in Streptococcus pneumoniae. Infect. Immun. **79:**4193–4200.
50. **Webb AJ, Homer KA, Hosie AH.** 2008. Two closely related ABC transporters in Streptococcus mutans are involved in disaccharide and/or oligosaccharide uptake. J. Bacteriol. **190:**168–178.
51. **Nunez-Samudio V, Chesneau O.** 2013. Functional interplay between the ATP-binding cassette Msr(D) protein and the membrane facilitator superfamily Mef(E) transporter for macrolide resistance in Escherichia coli. Res. Microbiol. **164:**226–235.
52. **Rees DC, Johnson E, Lewinson O.** 2009. ABC transporters: the power to change. Nat. Rev. Mol. Cell Biol. **10:**218–227.